

1 **Genomic detection of a secondary family burial in a single jar coffin in early Medieval Korea**

2
3 **Running title:** Ancient genomic detection of a family burial

4
5 **Authors:**

6 Don-Nyeong Lee¹, Chae Lin Jeon², Jiwon Kang³, Marta Burri⁴, Johannes Krause^{4,5}, Eun Jin Woo^{6,*},
7 Choongwon Jeong^{1,*}

8
9 **Affiliations:**

10 ¹ School of Biological Sciences, Seoul National University, Seoul, 08826, Republic of Korea

11 ² Department of Anthropology, Seoul National University, Seoul, 08826, Republic of Korea

12 ³ Central Institute of Cultural Heritage, Daejeon, 34029, Republic of Korea

13 ⁴ Max Planck Institute for the Science of Human History, Jena, 07745, Germany

14 ⁵ Max Planck Institute for Evolutionary Anthropology, Leipzig, 04103, Germany

15 ⁶ Department of History, Sejong University, Seoul, 05006, Republic of Korea

16
17 * **Correspondence to:** cwjeong@snu.ac.kr (C.J.), redqin@sejong.ac.kr (E.J.W.)

20 Abstract

21

22 **Objectives:** Family relationship is a key to understand the structure of past societies but its
23 archaeological reconstruction mostly stays circumstantial. Archaeogenetic information, especially
24 genome-wide data, provide an objective approach to accurately reconstruct the familial relationship of
25 ancient individuals, thus allowing a robust test of an archaeology-driven hypothesis of kinship. In this
26 study, we applied this approach to disentangle the genetic relationship of early Medieval individuals
27 from Korea, who were secondarily co-buried in a single jar coffin.

28 **Materials and Methods:** We obtained genome-wide data of six early Medieval Korean individuals
29 from a jar coffin. We inferred the genetic relatedness between these individuals and characterized their
30 genetic profiles using well-established population genetics methods.

31 **Results:** Congruent with the unusual pattern of multiple individuals in a single jar coffin, genome-wide
32 analysis of these individuals shows that they form an extended family, including a couple, their two
33 children and both paternal and maternal relatives. We show that these early Medieval Koreans have a
34 genetic profile similar to present-day Koreans.

35 **Discussion:** We show that an unusual case of a secondary multiple burial in a single jar coffin reflects
36 family relationship among the co-buried individuals. We find both paternal and maternal relatives co-
37 buried with the nuclear family, which may suggest a family structure with limited gender bias. We find
38 the genetic profile of early Medieval Koreans similar to that of present-day Koreans, suggesting no
39 substantial genetic shift in the Korean peninsula for the last 1,500 years.

40

41

42 Keywords

43 ancient DNA, family burial, jar coffin, Gusan Dangbuk-ri, population genomics

44

45

46 Research Highlights

- 47 ● Ancient genome-wide data find a family buried together in a jar coffin in early Medieval
48 Korea.
- 49 ● These early Medieval Koreans have a genetic profile similar to present-day Koreans.

50

51

52 Introduction

53

54 The burial practice using jar coffins was widespread throughout past societies in East Asia including
55 Southeast Asia, northern China, Manchuria, the Japanese archipelago, and the Korean Peninsula,
56 starting from the Neolithic period and continuing to the historic times (Bacvarov, 2006; Boeyens et al.,
57 2009; W. Kim, 1973; Shewan et al., 2020). In the Korean peninsula, while prehistoric and historic
58 burials with jar coffins are frequently found in all regions, they are most concentrated in the
59 southwestern Korea, such as Naju and Yeongam regions, during the 4-6th centuries AD (E.-J. Kim, 2021;
60 E. K. Kim, 2020; M. J. Kim et al., 2010; Oh, 2008; Park, 2010). Although burials with large, human-
61 height-scale jar coffins are famous, most jar coffins found in Korea are much smaller than human body.
62 Mostly, these small jar coffins host a single individual's skeleton secondarily collected after cremation.
63 The practice of cremation and the following secondary burial often result in a loss of some skeletal
64 elements, destruction of detailed morphological features that convey information on the sex, age, and
65 pathological history of the individual, and poor preservation of biological macromolecules such as
66 proteins and nucleic acids. For this reason, skeletal remains from the jar coffins have not been actively
67 investigated in bioanthropological and archaeogenetic studies, leaving the characteristics of people
68 buried in the jar-coffins an open question.

69

70 The Dangbuk-ri archaeological site is located at Gusan city in the west coastal region of South Korea
71 (Figure 1). Excavated during Summer 2016, this site includes several burials of the early Medieval
72 period (5-7th century AD; or the "three kingdoms" period). Among the various types of burials is one
73 jar coffin burial housing skeletal remains of multiple individuals (Figure 2). Considering the burial
74 context, it is most likely that the skeletal elements of these individuals were collected secondarily into

75 this jar coffin and buried at the same time. This case is considered unusual because most jar coffin
76 burials house only one individual and because individuals in the other types of multiple burials in the
77 early Medieval Korea were usually added into the burial in a sequential manner over an extended period
78 of time (E.-J. Kim, 2021).

79

80 In this study, we investigated the genetic relatedness between these co-buried individuals and their
81 genetic profiles using genome-wide data. In addition to revealing the familial relationship among them,
82 we model their genetic profiles in terms of their relationship with ancient and present-day East Asian
83 populations, including present-day Koreans, in high-resolution by utilizing rich information in genome-
84 wide data.

85

86

87 **Materials and Methods**

88

89 ***Skeletal analysis***

90 All skeletons were macroscopically examined by the two authors (E.J.W and C.L.J). In order to estimate
91 the minimum number of individuals (MNI) in a jar, fragments were first identified by element type, and
92 conjoining process was conducted to refit fragments from the same bone. Identified elements were
93 classified as either adult or subadult according to the degree of dental development, long-bone
94 epiphyseal fusion, diaphyseal length, cranial size and cortical thickness. Bones with fully fused
95 epiphyses and within the adult-sized range elements were classified as adults. Meanwhile, skeletal
96 elements with unfused epiphyses and within the size range of the subadults were classified into the
97 subadult category. After the skeletal elements were sorted to individuals, age estimation was further
98 refined based on morphological features. The value of MNI was derived by sorting elements into lefts
99 and rights, and then taking the greatest number as the final estimate following a published protocol (T.
100 E. White, 1953). Severely fragmented skeletal elements such as ribs, vertebrae and phalanges were
101 excluded from calculating MNI due to uncertainty in siding. Then, visual pair-matching was conducted
102 to decide if principal limb bones were from a single individual through the comparison of right and left
103 elements. Finally, different parts of the skeletal elements were segregated into individuals based on the
104 examination of degenerative changes, articulation, robusticity, age, and sex, along with osteometric
105 sorting (Adams & Byrd, 2014).

106

107 The sex and age were estimated for each skeletal individual, based on the Standards for Data Collection
108 (Buikstra & Ubelaker, 1994; Ubelaker, 1999). Sex was estimated using morphological features of the
109 skull and robusticity of limb bones. We were unable to use the pelvis for sex estimation because most
110 pelvic elements in the jar-coffin were severely fragmented. The age at death of each individual was
111 estimated by dental attrition, number of antemortem tooth loss, cranial suture closure, degeneration of
112 the auricular surface and pubic symphyseal surface, and degenerative changes of joint in limb bones
113 and the vertebral column. The age of subadults was estimated using the degrees of tooth formation and
114 eruption, epiphyseal fusion or diaphyseal length (Buikstra & Ubelaker, 1994; T. D. White & Folkens,
115 2005).

116

117 ***Sampling of skeletal materials***

118 Sample selection was performed by E.J.W. and C.L.J. in the Bioanthropology laboratory (Department
119 of Anthropology, Seoul National University). As compact bones are preferred for ancient DNA analysis,
120 intact petrous parts of the temporal bone from seven individuals were chosen. Two out of nine
121 individuals were not included in the analysis since the temporal parts including petrous were not well
122 preserved. In case of five adults, the left petrous bone was selected, for two subadults, the right petrous
123 parts were sampled. The outer surface of the petrous pyramid inside the skull was ground with a 4.8
124 mm cutter burr attached to a Dremel 9100-21 Fortiflex 2.5-Amp Stationary Flex Shaft Precision Rotary
125 Tool (Dremel, Mount Prospect, IL). Then the inferior border of the cochlea was ground to create a small
126 opening into the osseous labyrinth (Sirak et al., 2017). Into this opening, a 3.2 mm engraving cutting
127 burr was applied in a circular motion to obtain bone powder. The powder was collected in a sterilized
128 paper foil and placed in a sterile 1.5 ml Eppendorf tube for DNA extraction.

129

130 ***Ancient DNA laboratory work and sequencing***

131 For each of the seven individuals, a double-strand double-indexed Illumina sequencing library was built
132 from metagenomics DNA extracted from 30-50 mg of bone powder. DNA extraction and library
133 preparation were performed using previously published protocols (Dabney et al., 2013). For library
134 preparation, a partial treatment of the uracil-DNA-glycosylase (UDG) enzyme was included following
135 a published protocol (Rohland et al., 2015) to confine deaminated bases to the ends of the reads. All
136 laboratory works up to library preparation step were performed in a dedicated ancient DNA (aDNA)
137 clean room facility of the Max Planck Institute for the Science of Human History (MPI-SHH), Jena,
138 Germany. For six of the seven individuals with sufficient levels of human DNA preservation, ranging
139 0.1-2.6%, two rounds of in-solution capture for 1.24 million ancestry-informative single nucleotide
140 polymorphisms (SNPs) (the “1240K” panel) was performed to enrich libraries (Mathieson et al., 2015).
141 All libraries were sequenced using single-end 76 base pair (bp) sequencing on the Illumina HiSeq 4000
142 platform following the manufacturer’s protocols.

144 ***Ancient DNA sequencing data processing and authentication***

145 aDNA sequencing data were processed using the EAGER v1.92.50 wrapper (Peltzer et al., 2016).
146 Within the EAGER wrapper, Illumina adapter sequences were first trimmed from raw reads using
147 AdapterRemoval v2.3.0 (Schubert et al., 2016). Adapter-trimmed reads of 30 bp or longer were mapped
148 to the human reference genome with decoy sequences (hs37d5) using the aln/samse modules in BWA
149 v0.7.17 with “-n 0.01” option (Li & Durbin, 2009). PCR duplicates were removed using DeDup v0.12.5
150 (Peltzer et al., 2016), assuming that both ends of the reads were known. Unique mapped reads with
151 Phred-scaled mapping quality score 30 or higher were kept using samtools v1.9 (Li et al., 2009). To
152 remove deamination-based misincorporations (5’ C>T and 3’ G>A), the first and last two bases of each
153 read were soft-masked using the trimBam module of bamUtils v1.0.14 (Jun et al., 2015). Finally,
154 pseudo-haploid genotype data were determined by randomly sampling a single high-quality base
155 (Phred-scaled base quality score 30 or higher) per site per individual using samtools mpileup and
156 pileupCaller v1.4.0.5 (downloaded from <https://github.com/stschiff/sequenceTools>). For C/T and G/A
157 SNPs, end-masked BAM files were used. For the remaining SNPs that are not affected by post-mortem
158 deamination, BAM files without end-masking were used to maximize sequence data usage. The
159 authenticity of sequence data was checked by multiple measures. First, chemical modifications typical
160 of aDNA molecules were tabulated using mapDamage v2.0.9 (Jonsson et al., 2013). Second,
161 mitochondrial DNA contamination was estimated using schmutzi v1.5.5.5 (Renaud et al., 2015). Third,
162 X chromosome-based estimation of nuclear DNA contamination was performed for four male
163 individuals using the contamination module of the ANGSD v0.929 program (Korneliussen et al., 2014).
164 Mitochondrial haplogroups were determined by applying the HaploGrep v2 program (Weissensteiner
165 et al., 2016) to the consensus sequences called by the log2fasta program in schmutzi with “-q10” filter.
166 Y haplogroups were determined using a modified version of the yHaplo program with “--ancStopThresh
167 10” option to prevent the root-to-tip search from halting in an internal branch due to missing data
168 (downloaded from <https://github.com/alexhbnr/yhaplo>) (Poznik, 2016).

170 ***Reprocessing of whole genome sequences of present-day Koreans***

171 We downloaded high-coverage whole genome sequencing data of 104 Koreans from the Ulsan city from
172 KoVariome data (ftp://biobio.org/Release/KPGP/KPGP_Data_2017_Release_Candidate/). For the
173 FASTQ files with the Phred-64 scale quality scores, we rescaled quality scores to the Phred-33 scale
174 using seqtk v1.3-r106 with “seqtk seq -VQ64” command (<https://github.com/lh3/seqtk>). We aligned
175 reads to the human reference genome (hs37d5) using the BWA mem program v0.7.17 with “-M” flag
176 (Li & Durbin, 2010). We kept properly aligned paired-end reads by applying “-f 0x0003” filter in
177 samtools view v1.9 (Li et al., 2009) and merged per-lane BAM files into per-individual ones using
178 samtools merge. We removed duplicates using Picard MarkDuplicates v2.20.0 (downloaded from
179 <https://broadinstitute.github.io/picard/>) and kept reads with Phred-scaled mapping quality score 25 or
180 higher. From these analysis-ready BAM files, we produced two genotype calls for the 1,233,013 SNPs
181 in the 1240K panel. First, we calculated genotype likelihoods for each individual using the
182 UnifiedGenotyper module of the Genome Analysis Toolkit (GATK) v3.8.1.0 (McKenna et al., 2010)
183 with the “--allSitesPLs” flag, calculated posterior genotype probability by multiplying genotype
184 likelihoods with the GATK default prior [0.9985, 0.0010, 0.0005], and took genotype calls with

185 posterior probability 0.900 or higher. Second, we randomly sampled a base with the Phred-scaled base
186 quality score 30 or higher from a read with mapping quality score 30 or higher per site per individual
187 to create a pseudo-haploid call that mimics the genotype calling procedure of low-coverage ancient
188 individuals. For this procedure, we used samtools mpileup and pileupCaller v1.4.0.5. We merged the
189 two genotype calls of present-day Ulsan Koreans with the genome-wide data of world-wide present-
190 day populations typed on the Affymetrix Axiom® Genome-Wide Human Origins 1 array
191 (“HumanOrigins”) and the 1240K dataset for downstream analyses. We determined genetic sex of each
192 individual by comparing coverage of sex chromosomes with autosomes calculated for the 1240K sites
193 using samtools depth (Figure S1). We detected genetic outliers by projecting Ulsan Koreans to the top
194 principal components calculated for 2,077 present-day Eurasian individuals using the smartpca program
195 v16000 in the EIGENSOFT package v7.2.1 (Patterson et al., 2006). For the remaining individuals, we
196 detected close relative pairs by calculating pairwise mismatch rate (PMR) for each pair using the
197 random haploid calls and by estimating kinship coefficients using the --Z-genome module in PLINK
198 v1.90b6.9 (Chang et al., 2015). We removed one individual from each relative pair up to the second-
199 degree relatives for the downstream group-based analyses (Figure S2; Table S1).

200

201 ***Data set compilation***

202 We merged genome-wide genotype data of 2,967 present-day individuals typed on the HumanOrigins
203 array (Jeong et al., 2019; Lazaridis et al., 2016; Patterson et al., 2012) with whole genome sequences
204 of 104 Koreans from Ulsan (J. Kim et al., 2018), six Gunsan jar coffin individuals from this study, and
205 previously published ancient individuals (Allentoft et al., 2015; Damgaard, Marchi, et al., 2018;
206 Damgaard, Martiniano, et al., 2018; Fu et al., 2014; Fu et al., 2016; Haber et al., 2017; Harney et al.,
207 2018; Jeong et al., 2016; Jeong et al., 2020; Jeong et al., 2018; Jones et al., 2015; Kanzawa-Kiriyama
208 et al., 2019; Krzewińska et al., 2018; Lazaridis et al., 2017; Lazaridis et al., 2016; Lazaridis et al., 2014;
209 Lipson et al., 2018; Mathieson et al., 2018; Mathieson et al., 2015; McColl et al., 2018; Moreno-Mayar
210 et al., 2018; Narasimhan et al., 2019; Ning et al., 2020; Raghavan, DeGiorgio, et al., 2014; Raghavan,
211 Skoglund, et al., 2014; Rasmussen et al., 2014; Rasmussen et al., 2010; Rasmussen et al., 2015; Sikora
212 et al., 2019; Unterlander et al., 2017; C.-C. Wang et al., 2020; T. Wang et al., 2021; M. A. Yang et al.,
213 2020; Melinda A Yang et al., 2017; Yu et al., 2020). We also merged present-day world-wide populations
214 genotyped on the 1240K sites (Mallick et al., 2016) with whole genome sequences of 104 Koreans from
215 Ulsan, six Gunsan jar coffin individuals from this study, and previously published ancient individuals
216 to produce 1240K dataset. We provide a list of analysis groups and individuals used for each analysis
217 (Table S2).

218

219 ***Principal component analysis***

220 We ran principal component analysis (PCA) with 2,077 present-day Eurasian individuals from
221 HumanOrigins dataset with the option “lsqproject: YES” using smartpca v16000 and projected the
222 remaining individuals on to the PCs, including the Gunsan jar coffin individuals, present-day Ulsan
223 Koreans, and other ancient East Asian individuals. For the East Asian-only PCA, we ran PCA with 455
224 present-day East Asian individuals including Ulsan Koreans with the option “lsqproject: YES” and
225 “shrinkmode: YES” using smartpca v16000 and projected the remaining individuals onto the PCs.

226

227 ***Genetic kinship analysis***

228 We calculated PMR between each pair of ancient Gunsan jar coffin individuals across the 1,150,639
229 autosomal SNPs in the 1240K panel. Each pair was covered by at least 66,442 SNPs. We estimated
230 probability of sharing 0, 1, and 2 alleles using lcMLkin v0.5.0 to distinguish between parent-offspring
231 and full sibling (Lipatov et al., 2015). For the group-based analyses, we removed first-degree relatives
232 and kept three individuals (GUC002, GUC003, GUC005) with minimal genetic relatedness (Table S3)

233

234 ***Runs of Homozygosity analysis***

235 We investigated the runs of homozygosity (ROH) segments within the genome of each Gunsan jar coffin
236 individual to understand parental relatedness using hapROH (downloaded from
237 <https://pypi.org/project/hapROH/> v0.3a1) (Ringbauer et al., 2020). We analyze individuals whose SNPs
238 covered over 400,000 sites among 1240K sites at least once as recommended.

239

240 ***F-statistics and qpWave/qpAdm analysis***

241 We obtained f -statistics using 1240K dataset to maximize SNP coverage of ancient individuals. We
242 calculated outgroup- f_3 statistics of the form $f_3(\text{Mbuti}; \text{Gunsan jar coffin, world-wide})$ using qp3Pop
243 v650 to measure genetic affinity between two populations. We calculated f_4 statistics of the form
244 $f_4(\text{Mbuti, world-wide}; \text{Gunsan jar coffin, present-day Korean})$ using qpDstat v970 with the option
245 “f4mode: YES”. We used 121 present-day world-wide populations and 166 ancient populations for
246 these calculations (Table S2). We tested various admixture models of ancient and present-day East Asian
247 populations using qpWave v1200 and qpAdm v1201 programs in the AdmixTools v7.0 (Lazaridis et al.,
248 2016; Reich et al., 2012) on 1240K dataset. We used ten populations as an outgroup set (“right”
249 populations): central African Mbuti (Mbuti.DG; n=5), Early Neolithic farmers from western Anatolia
250 (Anatolia_N; n=23), Andamanese islanders Onge (Onge.DG; n=2), Neolithic Iranians from the Ganj
251 Dareh site (Iran_N; n=8), Epi-Paleolithic European hunter-gatherer from the Villabruna site (Villabruna;
252 n=1), a Late Pleistocene Native American individual from the Upward Sun River site in Alaska (USR1;
253 n=1), Early Neolithic hunter-gatherers from the western Baikal region (Baikal_EN; n=18), an Early
254 Neolithic individual from Shandong region in China (Boshan; n=1), an Early Neolithic individual from
255 the southern Chinese Liangdao site (Liangdao2; n=1), and Funadomari Jomon (Jomon_Funadomari;
256 n=2). We included “allsnps: NO” option.

257

258

259 **Results**

260

261 ***Archaeological context of the Gunsan jar coffin***

262 The Dangbuk-ri site is located in Gunsan, Jeollabuk-do province on the Korean peninsula (Figure 1).
263 The site was salvage excavated for the construction of a railroad line in 2016 by the Central Institute of
264 Cultural Heritage. The archaeological investigation was conducted during the period of approximately
265 60 days, starting from July 2016. Geographically the site was on the southern hillside of Mt. Dottae,
266 and it covered the top of a hill, the height of which was about 60 meters above sea level. A total of 21
267 burials were found at the Dangbuk-ri site. Among those burials, sixteen were the stone-cist type, four
268 burials were the stone-chamber type, and the remaining one was a jar coffin. Archaeological contexts,
269 such as burial types and artifacts, suggest that these burials are dated to the Woongjin period (475-538
270 AD) and the Sabi period (538-660 AD) of Baekje, corresponding to the early Medieval Three Kingdoms
271 Period.

272

273 The jar coffin burial was located on the southeastern hillside from the top, surrounded by stone-cist
274 burials and stone-chamber burials without any specific pattern. The jar was laid in a circular pit and two
275 stones were placed beside the jar to fix the jar body. At the time of discovery, the jar was found slanted
276 slightly. The mouth area of the jar has been broken without a cover of the coffin. In the jar coffin,
277 multiple skeletons were found together (Figure 2). No specific pattern was detected in the placement of
278 skeletal elements within the jar coffin, although more skulls were placed in the upper part of the jar. No
279 case of a sequential multiple burial (i.e. individuals were sequentially put to the jar coffin over an
280 extended time period) has been reported for this type of jar coffins, although there are cases with those
281 consisting of two jars. Also, individuals in this jar coffin were not separated into layers, a pattern
282 expected for a sequential multiple burial. Thus, multiple skeletons in the jar coffin are considered as
283 interred together approximately at the same time as a secondary burial. After finishing the excavation,
284 a pottery as a grave good was found at the bottom of a circular pit, implying that ritual behavior was
285 performed before laying the jar-coffin in state. The height of the jar, from the lower part of the jar to the
286 top is 72.3cm, the diameter is 32.1cm.

287

288 ***Ancient genome-wide data production***

289 We performed a genetic investigation of early Medieval individuals from Dangbuk-ri, Gunsan, in the
290 southwestern region of the Republic of Korea (Figure 1; Table 1). These individuals are dated to 5th to
291 7th century AD based on archaeological contexts and are found in a single jar coffin, with signatures of
292 secondary burial: multiple burials, either primary or secondary, within a single jar coffin are exceptional
293 given that most jar coffins host only a single individual. Based on the macroscopic examination of all
294 skeletal elements retrieved from the jar coffin, we determined MNI as nine, including six adults and

295 three subadults (Table 1). Following an in-solution capture protocol for ~1.2 million informative SNPs
296 (Mathieson et al., 2015), we obtained genome-wide data with on-target autosomal coverage ranging
297 0.2-1.8x and with 189K-764K on-target SNPs covered at least once for six individuals (Table 2). The
298 remaining three of nine individuals in the jar coffin did not yield sufficient genomic DNA to be analyzed.
299 All six individuals show post-mortem chemical damages typical of aDNA. All four males show nuclear
300 contamination < 2% based on their X chromosome data and five of six individuals have mitochondrial
301 contamination of 1-3%. Based on these measures, we included all six individuals into the downstream
302 analysis, including the one female without a contamination measure due to low mitochondrial coverage
303 (Table 2). For each individual, we called haploid genotypes across the 1240K panel SNPs by randomly
304 sampling a high-quality base. We concatenated their genotype data with published present-day and
305 ancient individuals on the HumanOrigins and the 1240K data sets for downstream analyses (Table S2)

306

307 *A familial relationship of individuals from a single jar coffin*

308 We first ran PCA of 2,077 present-day Eurasians and projected ancient individuals from the Gunsan jar
309 coffin onto the top PCs (Figure 3). All six individuals fall close to each other and to present-day Koreans,
310 suggesting no substantial genetic heterogeneity among them and an overall close relationship with
311 present-day Koreans (Figure 3). In the PCA of present-day East Asians including present-day Koreans,
312 the Gunsan jar coffin individuals also overlap with present-day Koreans (Figure S3).

313

314 Then we measured the genetic relatedness between these ancient individuals to test if the unusual
315 occasion of multiple individuals in a single jar coffin reflects their close relationship. Our estimates of
316 genetic relatedness based on genome-wide data indeed show that these individuals form a closely
317 related extended family: among 15 pairs combined from six individuals, we observe six first-degree,
318 two second-degree, and three third-degree relative pairs (Figure 4A; Table S3). Incorporating
319 mitochondrial and Y haplogroup information and age at death, we distinguish between parent-offspring
320 and full sibling pairs and propose most plausible pedigrees (Figure 4B). At the core of this pedigree is
321 a quartet family composed of a couple and their two children, one adult male and one subadult female.
322 Among the remaining two individuals, one male (GUC005) is the 1st degree relative of the mother of
323 the quartet (GUC004) and the 2nd degree relative of the two children (GUC001 and GUC007), but is
324 unrelated to the father (GUC002). The 1st degree relationship of GUC005 and GUC004 is likely a
325 parent-offspring one given the near-zero sharing of both alleles at the same SNP (Table S3). Both father-
326 daughter and mother-son relationship are compatible with genetic data: however, given that GUC005
327 and the quartet children share the identical mitochondrial haplogroup, we propose mother-son may be
328 more likely. That is, GUC005 and (GUC001, GUC007) may be half-siblings with the same mother.
329 Lastly, GUC003 is most likely a 3rd degree relative of the quartet father, sharing the same Y haplogroup.

330

331 We also investigated the distribution of ROH segments in three individuals with sufficient coverage (>
332 400K of 1240K SNPs are covered) using hapROH (Ringbauer et al., 2020). Finding few long ROH
333 segments (> 4 cM), we conclude that none of these individuals were the offspring of close relatives.

334

335 *The genetic profile of early Medieval Koreans*

336 To understand the genetic profile of the early Medieval Koreans from the Gunsan jar coffin, we first
337 measured the genetic affinity between the Gunsan jar coffin group and world-wide present-day and
338 ancient populations using outgroup- f_3 statistics of the form $f_3(\text{Mbuti}; \text{Gunsan jar coffin}, \text{world-wide})$.
339 As expected, the Gunsan jar coffin group shows the highest genetic affinity with present-day Koreans
340 (Figure. S4). Formally testing the genetic symmetry of the early Medieval and present-day Koreans
341 using f_4 statistics of the form $f_4(\text{Mbuti}, \text{world-wide}; \text{Gunsan jar coffin}, \text{present-day Korean})$, only a few
342 groups break the symmetry without clear geographic distribution (Figure S5). To formally model the
343 genetic relationship between ancient and present-day Korean groups, we utilized qpAdm, which
344 summarizes multiple f_4 statistics to test if a mixture of allele frequency of the chosen source populations
345 can accurately mimic that of the target population (Lazaridis et al., 2016; Reich et al., 2012). We find
346 that the present-day Koreans from Ulsan city (n=88) are adequately modeled as a mixture of Gunsan
347 jar coffin group and a European source with a small negative coefficient (-1.0% to -1.4%; Table S4A).
348 Reciprocally, Gunsan jar coffin group is modeled as a mixture of present-day Ulsan Koreans and a small
349 contribution from a European source (1.0-1.4%; Table S4A). We interpret these results as a technical

350 artifact rather than a signal of true admixture, considering a comparable amount of nuclear
351 contamination in Gunsan individuals (0.2-1.8%) and the small reference bias introduced during the read
352 mapping step.

353

354 To compare the genetic profiles of the ancient and present-day Koreans with populations of the
355 surrounding regions in a broader sense, we searched for distal admixture models that were commonly
356 applicable to those populations. We find that the Gunsan jar coffin individuals, present-day Koreans,
357 and various ancient groups from northern China are adequately positioned along the genetic north-south
358 cline in East Asia, within the range defined by the following two populations: i) Bronze Age individuals
359 from the Longtoushan archaeological site of the West Liao River region in the Upper Xiajiadian culture
360 context (“WLR_BA”) as a genetic northern proxy, and ii) Late Neolithic individuals from the Xitoucun
361 site in southern China (“Xitoucun”) as a genetic southern proxy (Figure 5; Table S5A). In both ancient
362 and present-day Koreans, we do not detect a statistically significant contribution from the Jomon hunter-
363 gatherer gene pool of the Japanese archipelago (Table S5A), although previous studies report occasional
364 presence of the Jomon ancestry contribution from Neolithic to the early Medieval period (Gelabert et
365 al., 2021; Robbeets et al., 2021). When we replace the genetic northern proxy from WLR_BA to Middle
366 Neolithic individuals from the Miaozigou site in Inner Mongolia (“Miaozigou_MN”), we detect a small
367 but significant amount of Jomon contribution in the Gunsan individuals and present-day Ulsan Koreans
368 (3.1-4.4%; Table S5B). We believe that WLR_BA provides a more suitable model for ancient and
369 present-day Koreans given its geographical and temporal proximity to them.

370

371

372 Discussion

373

374 We present a genomic study of individuals from the Gunsan jar coffin, an unusual case of a secondary
375 multiple burial where at least nine individuals were co-buried in a single small jar coffin. We confirm
376 our hypothesis that this unusual burial represents an unusual relationship among the co-buried
377 individuals, i.e. an extended family, including a core of a couple and their two children, as well as both
378 paternal and maternal relatives. The inferred pedigree may imply little gender bias in the family
379 structure of early Medieval Koreans lived in the area. Further archaeogenomic studies on the ancient
380 individuals excavated from an unusual burial context or those from a single cemetery will provide more
381 insights into past mortuary practices and social structures.

382

383 While the genetic origins of present-day Koreans have not been fully understood due to lack of relevant
384 ancient genome data, individuals from the Gunsan jar coffin provide among the first past human genetic
385 profiles in ancient Korea. Since this type of small jar coffins are considered to be associated with
386 commoners rather than with sociopolitical elites, the Gunsan jar coffin individuals provide a glimpse
387 on the genetic profile of the general population of the early Medieval Korea, albeit small in number.
388 Our population genomic analysis shows a long-term presence of the genetic profile of present-day
389 Koreans in the Korean peninsula at least since the early Medieval period. However, this does not imply
390 a complete genetic isolation of the Korean population from their neighbors over the last two millennia.
391 On the contrary, there are a growing body of genetic evidence supporting high connectivity between
392 proto-historic Korea and its neighboring regions: a recent study reported a few early Medieval
393 individuals with a substantial level of the Jomon ancestry from the Japanese archipelago (Gelabert et
394 al., 2021), suggesting a vibrant international network supporting movements of people and goods.
395 Furthermore, Kofun-period individuals from Japan suggests a continued gene flow from the continental
396 East Asia with the Korean peninsula as a highly likely source region (Cooke et al., 2021). Further
397 archaeogenetic studies on proto-historic sites in and around the Korean peninsula will help us accurately
398 delineate the networks between the past East Asian societies.

399

400

401 Acknowledgements

402

403 This work was supported by the National Research Foundation of Korea grant funded by the Korea
404 government (No. 2018R1A5A7023490 to E.J.W. and 2020R1C1C1003879 to C.J.) and the Max Planck

405 Society.

406

407

408 **Data Availability**

409

410 The raw DNA sequences (FASTQ) and the alignment data (BAM) reported in this paper have been
411 deposited in the European Nucleotide Archive under the accession number PRJEB51247. Data will be
412 made publicly available when the manuscript is published.

413

414

415 **Conflict of Interest Statement**

416

417 The authors declare no conflict of interest.

418

419

420 **Table 1. Summary of morphological examination of the skeletal elements found in the Gunsan jar**
 421 **coffin.** (A) Estimation of MNI based on the number of skeletal elements. We detected at least six adult
 422 individuals and three subadults, totaling at least nine individuals in the jar coffin. Because of incomplete
 423 preservation of skeletal elements per individual, per-element MNI is smaller than the MNI based on all
 424 elements. (B) Estimation of sex and age of each individual.
 425

A. Estimation of MNI					
Element	Adult		Subadult		MNI
	Right	Left	Right	Left	
Cranium					
<i>Frontal</i>		6		2	8
<i>Parietal</i>	6	6	2	1	8
<i>Temporal</i>	6	6	2	2	8
<i>Occipital</i>		6		1	7
Maxilla	5	3	1	1	6
Mandible	4	5	2	1	7
Clavicle	5	4	0	0	5
Scapula	5	5	0	0	5
Humerus	5	5	3	2	8
Radius	5	4	2	1	7
Ulna	5	5	3	2	8
Os coxae	6	5	2	0	8
Femur	5	5	3	3	8
Tibia	5	5	2	3	8
Fibula	5	5	0	0	5

B. Estimation of sex and age			
Age category	ID	Skeletal sex	Age at death
Adult	01	F	50+ years
	02	M	36-50 years
	03	F	21-35 years
	04	F	Adult
	05	M	36-50 years
	06	Probably F	21-35 years
Subadult	07	Indeterminable	2-4 years
	08	Indeterminable	6-10 years
	09	Indeterminable	15-18 years

426
 427

428

429 **Table 2. A summary of sequencing and genetic information of six ancient individuals in this study.**
 430 Six of the seven individuals yield sufficient human DNA for genome-wide analysis. The numbers of
 431 covered target sites are counted among 1,233,013 SNPs in the 1240K panel and 593,124 autosomal
 432 SNPs in the HumanOrigins panel. X-chromosome based contamination estimates represent the point
 433 estimate ± 1 s.e.m., and mitochondrial estimates represent the point estimate and the 95% credible
 434 interval.

435

Lab ID	ID	Genetic Sex	Pre-capture % human DNA	Post-capture % target reads	# of reads sequenced	# of uniquely mapped reads
GUC001	01; skull 1	M	0.129	2.45	36,063,678	1,169,573
GUC002	02; skull 2	M	1.219	14.90	25,871,919	5,363,973
GUC003	03; skull 3	M	0.307	4.99	32,502,379	2,076,521
GUC004	04; skull 4	F	0.350	6.89	36,179,211	2,592,575
GUC005	06; skull 6	M	2.624	22.91	20,992,582	6,805,731
GUC007	09; subadult 3	F	1.656	18.35	24,249,836	5,438,347
GUC006	08; subadult 2	N/A	0.030	Fail	N/A	N/A

Lab ID	Lat	Lon	Coverage				# of covered target sites	
			Autosome	X	Y	MT	1240K	HumanOrigins
GUC001	35.94038889	126.7141944	0.195	0.075	0.091	0.54	189,920	96,738
GUC002	35.94038889	126.7141944	1.097	0.420	0.518	3.11	639,758	327,372
GUC003	35.94038889	126.7141944	0.312	0.122	0.147	0.48	284,857	144,896
GUC004	35.94038889	126.7141944	0.397	0.304	0.004	0.56	342,704	174,677
GUC005	35.94038889	126.7141944	1.839	0.698	0.939	2.17	764,537	389,635
GUC007	35.94038889	126.7141944	1.087	0.812	0.015	2.22	643,530	330,307

Lab ID	Post-mortem damage		Contamination estimates		Uniparental haplogroup	
	5' C>T	3' G>A	X	MT	MT	Y
GUC001	0.2928	0.2819	0.0184 \pm 0.0147	0.01 (0.00-0.02)	D4c1b1	Q1a (Q-L472)
GUC002	0.2096	0.1952	0.0020 \pm 0.0017	0.01 (0.00-0.02)	D4b2b1	Q1a1a1 (Q-M120)
GUC003	0.2623	0.2575	0.0106 \pm 0.0073	0.01 (0.00-0.02)	B5b3a	Q1a1 (Q-F1251)
GUC004	0.2413	0.2376	N/A	N/A	N/A	-
GUC005	0.2140	0.2012	0.0058 \pm 0.0016	0.03 (0.01-0.05)	D4c1b1	O1b2a2a1a (O-CTS7620)
GUC007	0.2328	0.2119	N/A	0.02 (0.00-0.04)	D4c1b1	-

436
 437



438

439

440

441

442

443

444

445

446

447

448

449

450

451

452

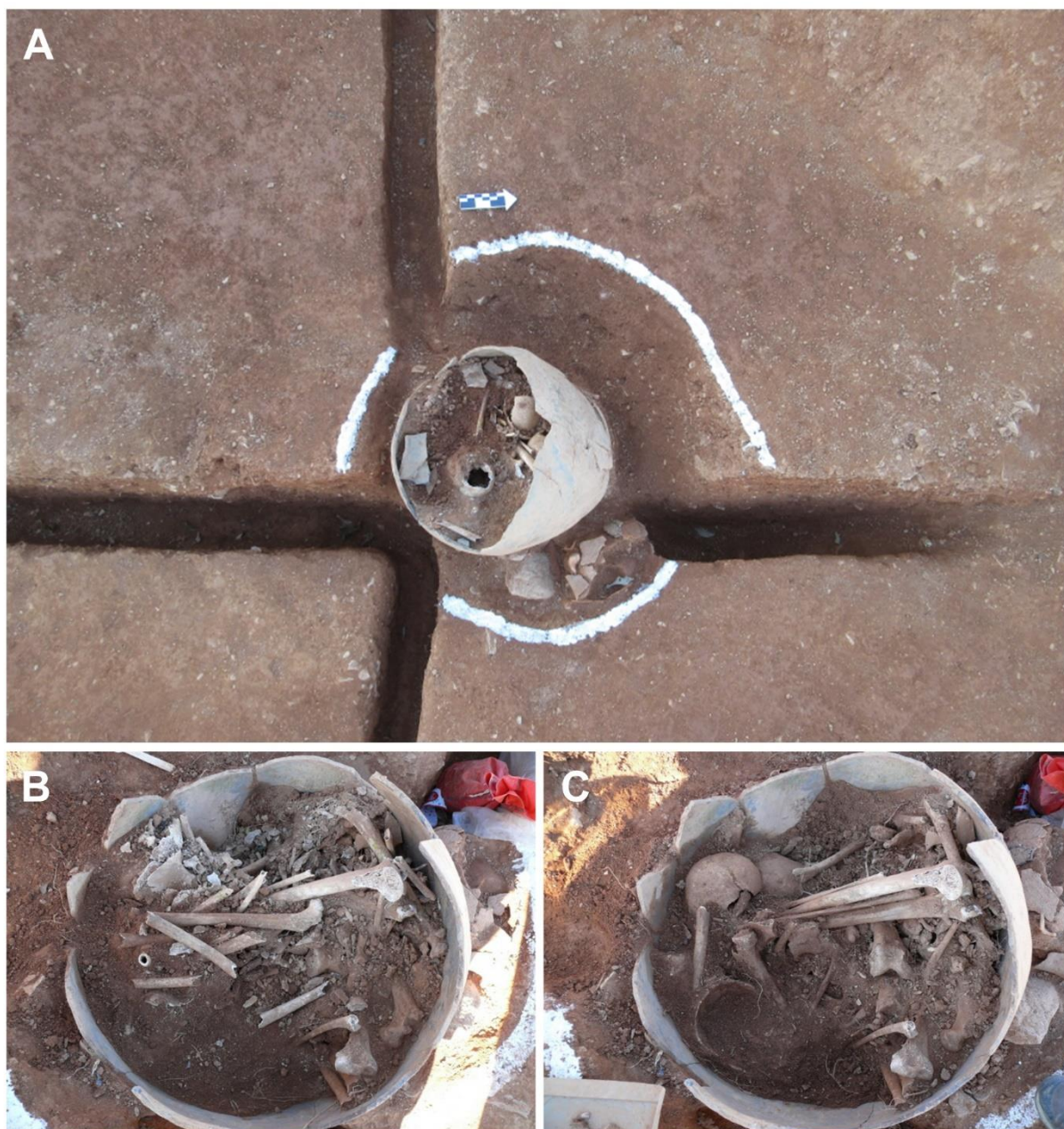
453

454

455

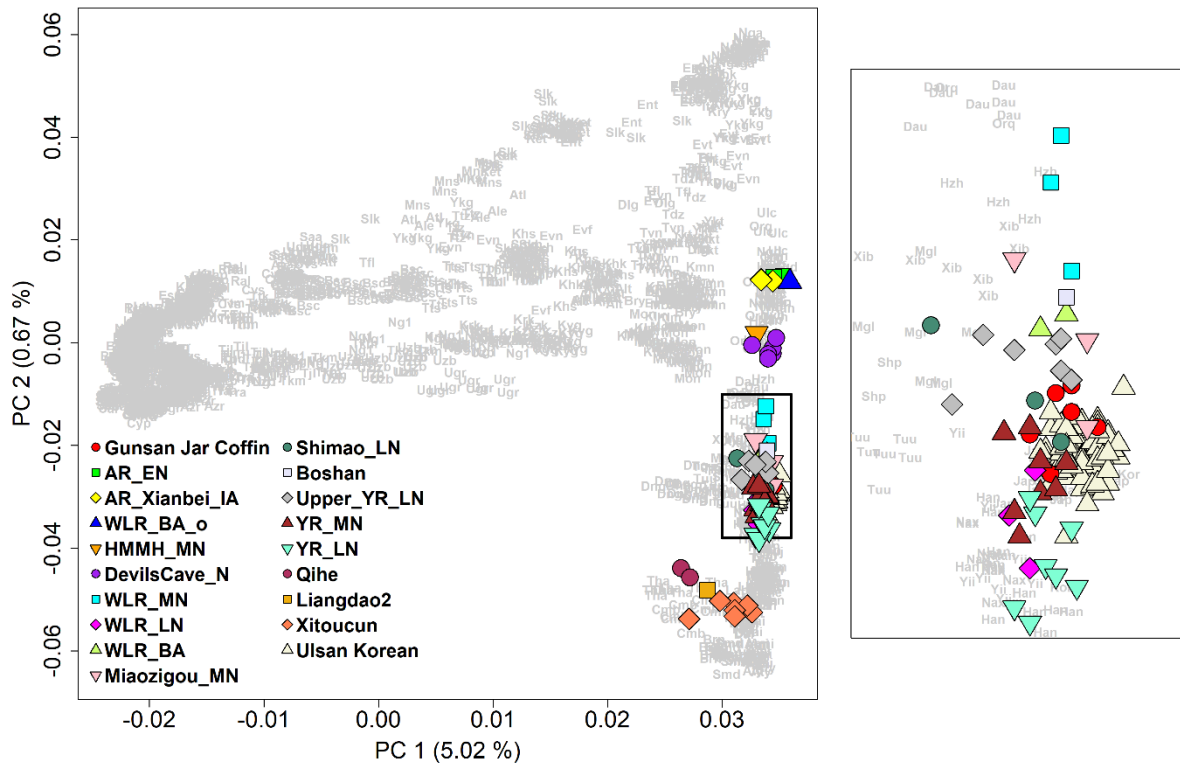
456

Figure 1. The geographic location of the key ancient and present-day populations used in this study. Except for present-day Ulsan Koreans from southeastern Korea, all the other groups marked on the map represent ancient East Asian groups. The base map is produced using the Natural Earth public domain map dataset (<https://www.naturalearthdata.com/downloads/10m-raster-data/10m-cross-blend-hypso/>). AR_EN = Amur River Early Neolithic individuals from the Zhalainuoer/Wuqi site; AR_Xianbei_IA = Amur River Iron Age individuals from the Xianbei context of the Mogushan site; Boshan = an early Neolithic individual from Shandong region; DevilsCave_N = Early Neolithic individuals from the Russian Far East; HMMH_MN = Middle Neolithic individual from the Haminmangha site; Liangdao2 = an Early Neolithic individual from the Liangdao site; Miaozigou_MN = Middle Neolithic individuals from the Miaozigou site; Qihe = Early Neolithic individuals from the Qihe site; Shimao_LN = Late Neolithic individuals from the Shengedaliang site; Upper_YR_LN = Upper Yellow River Late Neolithic individuals from the Jinchankou and Lajia sites; WLR_MN = West Liao River Middle Neolithic individuals from the Banlashan site; WLR_LN = WLR Late Neolithic individuals from the Erdaojingzi site; WLR_BA/WLR_BA_o = WLR Bronze Age individuals from the Longtoushan site; Xitoucun = Late Neolithic individuals from the Xitoucun site; YR_MN = Yellow River Middle Neolithic individuals from the Xiaowu and Wanggou site; YR_LN = YR Late Neolithic individuals from the Haojiatai/Pingliangtai/Wadian site.



457
458
459
460

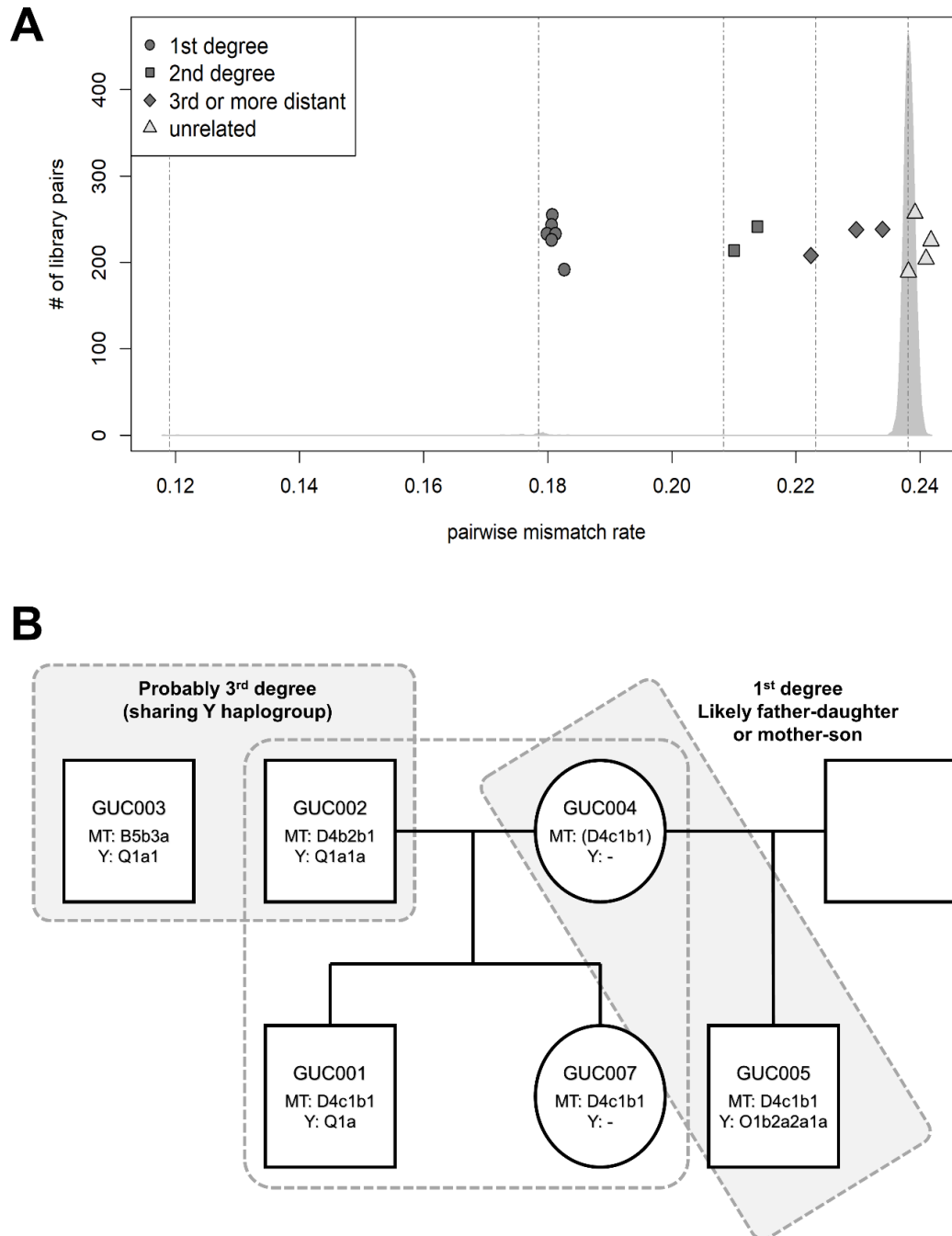
Figure 2. Revealed skeletons in a jar-coffin, Dangbuk-ri site *in situ*. (A) A wide view of the Gunsan jar-coffin. (B, C) The remains of the Gunsan jar-coffin individuals.



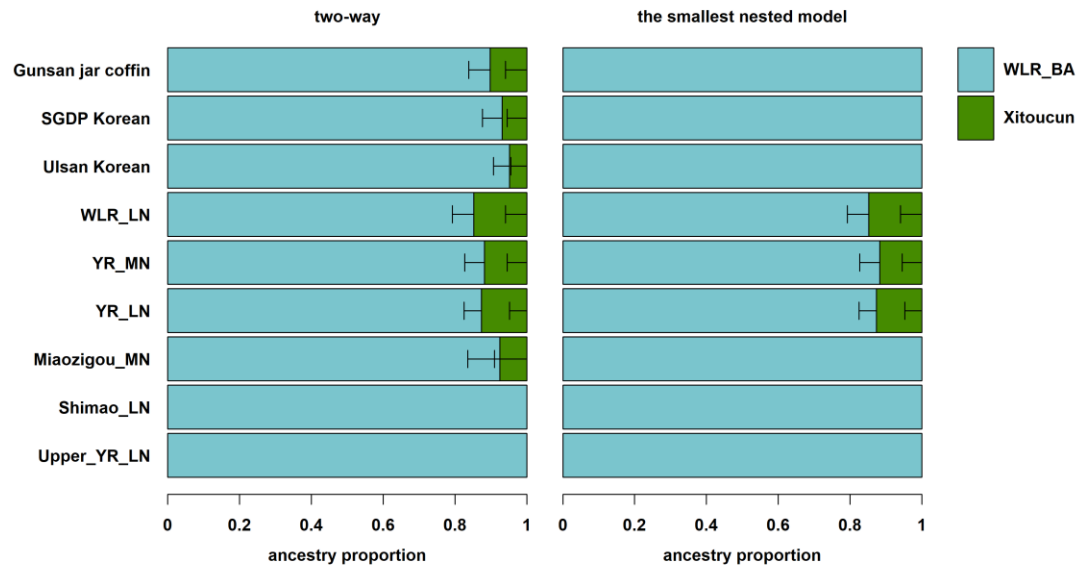
Abz Abazin; Abk Abkhasian; Adg Adygei; Abn Albanian; Ale Aleut; Atl Aleut_Tlingit; Alt Altaian; Ack Altaian_Chelkans; Ami Ami; Arm Armenian; Ahm Armenian_Hemsheni; Aty Atayal; Avr Avar; Azr Azeri; Blk Balkar; Bsc Bashkir; Bsq Basque; Blr Belarusian; Bes Besermyan; Brn Borneo; Blg Bulgarian; Bry Buryat; Cmb Cambodian; Cch Chechen; Chk Chukchi; Cvs Chuvash; Ccs Circassian; Crt Croatian; Cyp Cypriot; Cze Czech; Dai Dai; Drg Darginian; Dau Daur; Dlg Dolgan; Dng Dungan; Ent Enets; Eng English; Ecs Eskimo_CS; Enk Eskimo_NK; Est Estonian; Evn Even; Evf Evenk_FarEast; Evt Evenk_Transbaikal; Ezd Ezid; Fin Finnish; Fre French; Ggz Gagauz; Grg Georgian; Ger German; Grk Greek; Han Han; Hzh Hezhen; Hun Hungarian; Ice Icelandic; Igs Ingushian; Iri Irish; Iru Irish_Ulster; Itn Italian_North; Its Italian_South; Itl Itelmen; Jap Japanese; Jas Jew_Ashkenazi; Jgr Jew_Georgian; Kbd Kabardinian; Ktg Kaitag; Klk Kalmyk; Krc Karachai; Krk Karakalpak; Krl Karelian; Kzk Kazakh; Ket Ket; Khs Khakass; Khk Khakass_Kachins; Kmn Khamnegan; Kin Kinh; Kor Korean; Kry Koryak; Kbc Kubachinian; Kmk Kumyk; Krd Kurd; Kyg Kyrgyz; Lah Lahu; Lak Lak; Lzg Lezgin; Lth Lithuanian; Mlt Maltese; Mns Mansi; Mia Miao; Mld Moldavian; Mon Mongol; Mgl Mongola; Mdv Mordovian; Nan Nanai; Nax Naxi; Ngd Negidal; Nga Nganasan; Nvh Nivh; Ng1 Nogai; Nwg Norwegian; Orc Orcadian; Orq Oroqen; Ost Ossetian; Pol Polish; Rom Romanian; Rus Russian; Rak Russian_Krasnoborsky; Ral Russian_Leshukonsky; Rap Russian_Pinezhsy; Saa Saami; Sar Sardinian; Sct Scottish; Sik Selkup; Smd Semende; She She; Shp Sherpa; Sst Shetlandic; Skh Shor_Khakassia; Smn Shor_Mountain; Scl Sicilian; Srb Sorb; Spa Spanish; Spn Spanish_North; Tbs Tabasaran; Tjl Tajik; Ttk Tatar_Kazan; Ttm Tatar_Mishar; Tts Tatar_Siberian; Ttz Tatar_Zabolotniye; Tha Thai; Tib Tibetan; Tdz Todzin; Tfi Tofalar; Tuu Tu; Tbl Tubalar; Tuj Tujia; Tra Turkish; Trb Turkish_Balikesir; Tkm Turkmen; Tvn Tuvanian; Udm Udmurt; Ukr Ukrainian; Ulc Ulchi; Ugr Uygur; Uzb Uzbek; Vep Veps; Xib Xibo; Ykt Yakut; Yii Yi; Ykg Yukagir

461
462
463
464
465
466

Figure 3. Principal component analysis from 2,077 present-day Eurasian individuals. We project the Gunsan jar coffin and other ancient East Asian individuals and present-day Koreans from Ulsan (marked by color-filled shapes) onto the top two PCs calculated for 2,077 present-day Eurasian individuals (marked by three-letter codes). Present-day and ancient Koreans fall on top of each other.



467
 468 **Figure 4. Genetic relationship of the six Gusan jar coffin individuals.** (A) We show the estimated
 469 genetic relatedness of 15 pairs of the Gusan jar coffin individuals with the pairwise mismatch rate of
 470 genotypes (color-filled shapes). On the background, we plot the density of the pairwise mismatch rate
 471 values of 102 present-day Ulsan Koreans. Dotted vertical lines represent the expected pairwise
 472 mismatch rate of the identical, 1st degree, 2nd degree, 3rd degree relatives and the unrelated pairs of
 473 present-day Koreans, from left to right, respectively. Gusan jar coffin individuals show slightly higher
 474 pairwise mismatch rate values than the present-day Koreans. (B) A reconstruction of the pedigree of the
 475 six Gusan jar coffin individuals. MT and Y represent the corresponding uniparental haplogroups.
 476 GUC004 and GUC005 are the 1st degree relatives that are likely mother-son or father-daughter. Here
 477 we show a mother-son relationship based on the shared MT haplotype between GUC005 and (GUC001,
 478 GUC007), offspring of GUC004.
 479



480
481
482
483
484
485
486
487

Figure 5. QpAdm modeling of Gunsan jar coffin and other ancient and present-day East Asian populations. We show the results of a two-way admixture model of WLR_BA+Xitoucun on the left side and the results of its smallest sub-model after removing all components that do not significantly increase model fit on the right side (Table S5A). Horizontal bars represent the standard error measure (s.e.m.) of ancestry proportion estimates, calculated by the 5cM block jackknifing procedure as implemented in the qpAdm program.

References

- 488
489
490 Adams, B., & Byrd, J. (2014). *Commingle human remains: methods in recovery, analysis, and*
491 *identification*. Amsterdam: Academic Press.
- 492 Allentoft, M. E., Sikora, M., Sjogren, K. G., Rasmussen, S., Rasmussen, M., Stenderup, J., . . .
493 Willerslev, E. (2015). Population genomics of bronze age Eurasia. *Nature*, *522*(7555), 167-172.
494 doi:<https://doi.org/10.1038/nature14507>
- 495 Bacvarov, K. (2006). Early Neolithic jar burials in southeast Europe: a comparative approach.
496 *Documenta Praehistorica*, *33*, 101-106. doi:<https://doi.org/10.4312/dp.33.11>
- 497 Boeyens, J., Van der Ryst, M., Coetzee, F., Steyn, M., & Loots, M. (2009). From uterus to jar: the
498 significance of an infant pot burial from Melora Saddle, an early nineteenth-century African
499 farmer site on the Waterberg Plateau. *Southern African Humanities*, *21*(1), 213-238.
- 500 Buikstra, J. E., & Ubelaker, D. H. (1994). *Standards for data collection from human skeletal remains:*
501 *Proceedings of a seminar at the Field Museum of natural history*. Fayetteville: Arkansas:
502 Arkansas archeological survey research series no 44.
- 503 Chang, C. C., Chow, C. C., Tellier, L. C., Vattikuti, S., Purcell, S. M., & Lee, J. J. (2015). Second-
504 generation PLINK: rising to the challenge of larger and richer datasets. *Gigascience*, *4*(1), 7.
505 doi:<https://doi.org/10.1186/s13742-015-0047-8>
- 506 Cooke, N. P., Mattiangeli, V., Cassidy, L. M., Okazaki, K., Stokes, C. A., Onbe, S., . . . Nakagome, S.
507 (2021). Ancient genomics reveals tripartite origins of Japanese populations. *Science Advances*,
508 *7*(38), eabh2419. doi:<https://doi.org/10.1126/sciadv.abh2419>
- 509 Dabney, J., Knapp, M., Glocke, I., Gansauge, M. T., Weihmann, A., Nickel, B., . . . Meyer, M. (2013).
510 Complete mitochondrial genome sequence of a Middle Pleistocene cave bear reconstructed
511 from ultrashort DNA fragments. *Proceedings of the National Academy of Sciences*, *110*(39),
512 15758-15763. doi:<https://doi.org/10.1073/pnas.1314445110>
- 513 Damgaard, P. B., Marchi, N., Rasmussen, S., Peyrot, M., Renaud, G., Korneliusen, T., . . . Willerslev,
514 E. (2018). 137 ancient human genomes from across the Eurasian steppes. *Nature*, *557*(7705),
515 369-374. doi:<https://doi.org/10.1038/s41586-018-0094-2>
- 516 Damgaard, P. B., Martiniano, R., Kamm, J., Moreno-Mayar, J. V., Kroonen, G., Peyrot, M., . . .
517 Baimukhanov, N. (2018). The first horse herders and the impact of early Bronze Age steppe
518 expansions into Asia. *Science*, *360*(6396), eaar7711.
519 doi:<https://doi.org/10.1126/science.aar7711>
- 520 Fu, Q., Li, H., Moorjani, P., Jay, F., Slepchenko, S. M., Bondarev, A. A., . . . Paabo, S. (2014). Genome
521 sequence of a 45,000-year-old modern human from western Siberia. *Nature*, *514*(7523), 445-
522 449. doi:<https://doi.org/10.1038/nature13810>
- 523 Fu, Q., Posth, C., Hajdinjak, M., Petr, M., Mallick, S., Fernandes, D., . . . Reich, D. (2016). The genetic
524 history of ice age Europe. *Nature*, *534*(7606), 200-205.
525 doi:<https://doi.org/10.1038/nature17993>
- 526 Gelabert, P., Blazyte, A., Chang, Y., Fernandes, D. M., Jeon, S., Hong, J. G., . . . Cheronet, O. (2021).
527 Diverse northern Asian and Jomon-related genetic structure discovered among socially
528 complex Three Kingdoms period Gaya region Koreans. *bioRxiv*.
529 doi:<https://doi.org/10.1101/2021.10.23.465563>
- 530 Haber, M., Doumet-Serhal, C., Scheib, C., Xue, Y., Danecek, P., Mezzavilla, M., . . . Tyler-Smith, C.
531 (2017). Continuity and admixture in the last five millennia of Levantine history from ancient
532 Canaanite and present-day Lebanese genome sequences. *The American Journal of Human*
533 *Genetics*, *101*(2), 274-282. doi:<https://doi.org/10.1016/j.ajhg.2017.06.013>
- 534 Harney, É., May, H., Shalem, D., Rohland, N., Mallick, S., Lazaridis, I., . . . Patterson, N. (2018).
535 Ancient DNA from Chalcolithic Israel reveals the role of population mixture in cultural
536 transformation. *Nature Communications*, *9*(1), 1-11. doi:[https://doi.org/10.1038/s41467-018-](https://doi.org/10.1038/s41467-018-05649-9)
537 [05649-9](https://doi.org/10.1038/s41467-018-05649-9)
- 538 Jeong, C., Balanovsky, O., Lukianova, E., Kahbatkyzy, N., Flegontov, P., Zaporozhchenko, V., . . .
539 Khussainova, E. (2019). The genetic history of admixture across inner Eurasia. *Nature Ecology*
540 *& Evolution*, *3*(6), 966-976. doi:<https://doi.org/10.1038/s41559-019-0878-2>
- 541 Jeong, C., Ozga, A. T., Witonsky, D. B., Malmstrom, H., Edlund, H., Hofman, C. A., . . . Warinner, C.

- 542 (2016). Long-term genetic stability and a high-altitude East Asian origin for the peoples of the
543 high valleys of the Himalayan arc. *Proceedings of the National Academy of Sciences*, 113(27),
544 7485-7490. doi:<https://doi.org/10.1073/pnas.1520844113>
- 545 Jeong, C., Wang, K., Wilkin, S., Taylor, W. T. T., Miller, B. K., Bemmman, J. H., . . . Warinner, C. (2020).
546 A dynamic 6,000-year genetic history of Eurasia's Eastern Steppe. *Cell*, 183(4), 890-904.
547 doi:<https://doi.org/10.1016/j.cell.2020.10.015>
- 548 Jeong, C., Wilkin, S., Amgalantugs, T., Bouwman, A. S., Taylor, W. T. T., Hagan, R. W., . . . Warinner,
549 C. (2018). Bronze Age population dynamics and the rise of dairy pastoralism on the eastern
550 Eurasian steppe. *Proceedings of the National Academy of Sciences*, 115(48), E11248-E11255.
551 doi:<https://doi.org/10.1073/pnas.1813608115>
- 552 Jones, E. R., Gonzalez-Fortes, G., Connell, S., Siska, V., Eriksson, A., Martiniano, R., . . . Bradley, D.
553 G. (2015). Upper Palaeolithic genomes reveal deep roots of modern Eurasians. *Nature*
554 *Communications*, 6(1), 1-8. doi:<https://doi.org/10.1038/ncomms9912>
- 555 Jonsson, H., Ginolhac, A., Schubert, M., Johnson, P. L., & Orlando, L. (2013). mapDamage2.0: fast
556 approximate Bayesian estimates of ancient DNA damage parameters. *Bioinformatics*, 29(13),
557 1682-1684. doi:<https://doi.org/10.1093/bioinformatics/btt193>
- 558 Jun, G., Wing, M. K., Abecasis, G. R., & Kang, H. M. (2015). An efficient and scalable analysis
559 framework for variant extraction and refinement from population-scale DNA sequence data.
560 *Genome Research*, 25(6), 918-925. doi:<https://doi.org/10.1101/gr.176552.114>
- 561 Kanzawa-Kiriyama, H., Jinam, T. A., Kawai, Y., Sato, T., Hosomichi, K., Tajima, A., . . . Saitou, N.
562 (2019). Late Jomon male and female genome sequences from the Funadomari site in Hokkaido,
563 Japan. *Anthropological Science*, 127(2), 83-108. doi:<https://doi.org/10.1537/ase.190415>
- 564 Kim, E.-J. (2021). A study on the character of the funerary practices and the occupants of the jar coffins
565 in the Yeongsan river basin. *Journal of The Honam Archaeological Society Honam KoKo -*
566 *Hakbo*, 68(0), 40-64. doi:<https://doi.org/10.55473/JHAS.2021.68.40> Korean.
- 567 Kim, E. K. (2020). The Construction and the funeral rites for a Jar Coffin Tombs in Silla Area. *The*
568 *Journal of Korean Field Archaeology*, 39, 5-40. doi:<https://doi.org/10.35347/jkfa.2020..39.5>
569 Korean.
- 570 Kim, J., Weber, J. A., Jho, S., Jang, J., Jun, J., Cho, Y. S., . . . Bhak, J. (2018). KoVariome: Korean
571 National Standard Reference Variome database of whole genomes with comprehensive SNV,
572 indel, CNV, and SV analyses. *Scientific Reports*, 8(1), 5677.
573 doi:<https://doi.org/10.1038/s41598-018-23837-x>
- 574 Kim, M. J., Kim, Y. S., Oh, C. S., Lee, S. J., Bok, G. D., Yi, Y. S., . . . Shin, D. H. (2010). Anthropological
575 study on ancient human skull and teeth discovered from urn coffin of Proto-Three Kingdoms
576 period in Korea. *Korean Journal of Physical Anthropology*, 23(4), 169-175. Korean.
- 577 Kim, W. (1973). *Opening of Korean archaeology*. Seoul: Ilchokak. Korean.
- 578 Korneliussen, T. S., Albrechtsen, A., & Nielsen, R. (2014). ANGSD: analysis of next generation
579 sequencing data. *BMC Bioinformatics*, 15(1), 1-13. doi:[https://doi.org/10.1186/s12859-014-](https://doi.org/10.1186/s12859-014-0356-4)
580 [0356-4](https://doi.org/10.1186/s12859-014-0356-4)
- 581 Krzewińska, M., Kılınc, G. M., Juras, A., Koptekin, D., Chyleński, M., Nikitin, A. G., . . . Kraeva, L.
582 (2018). Ancient genomes suggest the eastern Pontic-Caspian steppe as the source of western
583 Iron Age nomads. *Science Advances*, 4(10), eaat4457.
584 doi:<https://doi.org/10.1126/sciadv.aat4457>
- 585 Lazaridis, I., Mittnik, A., Patterson, N., Mallick, S., Rohland, N., Pfrengle, S., . . . Stamatoyannopoulos,
586 G. (2017). Genetic origins of the Minoans and Mycenaeans. *Nature*, 548(7666), 214-218.
587 doi:<https://doi.org/10.1038/nature23310>
- 588 Lazaridis, I., Nadel, D., Rollefson, G., Merrett, D. C., Rohland, N., Mallick, S., . . . Sirak, K. (2016).
589 Genomic insights into the origin of farming in the ancient Near East. *Nature*, 536(7617), 419-
590 424. doi:<https://doi.org/10.1038/nature19310>
- 591 Lazaridis, I., Patterson, N., Mittnik, A., Renaud, G., Mallick, S., Kirsanow, K., . . . Krause, J. (2014).
592 Ancient human genomes suggest three ancestral populations for present-day Europeans. *Nature*,
593 513(7518), 409-413. doi:<https://doi.org/10.1038/nature13673>
- 594 Li, H., & Durbin, R. (2009). Fast and accurate short read alignment with Burrows-Wheeler transform.
595 *Bioinformatics*, 25(14), 1754-1760. doi:<https://doi.org/10.1093/bioinformatics/btp324>
- 596 Li, H., & Durbin, R. (2010). Fast and accurate long-read alignment with Burrows-Wheeler transform.

- 597 *Bioinformatics*, 26(5), 589-595. doi:<https://doi.org/10.1093/bioinformatics/btp698>
- 598 Li, H., Handsaker, B., Wysoker, A., Fennell, T., Ruan, J., Homer, N., . . . Genome Project Data
599 Processing, S. (2009). The sequence alignment/map format and SAMtools. *Bioinformatics*,
600 25(16), 2078-2079. doi:<https://doi.org/10.1093/bioinformatics/btp352>
- 601 Lipatov, M., Sanjeev, K., Patro, R., & Veeramah, K. R. (2015). Maximum likelihood estimation of
602 biological relatedness from low coverage sequencing data. *bioRxiv*.
603 doi:<https://doi.org/10.1101/023374>
- 604 Lipson, M., Cheronet, O., Mallick, S., Rohland, N., Oxenham, M., Pietrusewsky, M., . . . Reich, D.
605 (2018). Ancient genomes document multiple waves of migration in Southeast Asian prehistory.
606 *Science*, 361(6397), 92-95. doi:<https://doi.org/10.1126/science.aat3188>
- 607 Mallick, S., Li, H., Lipson, M., Mathieson, I., Gymrek, M., Racimo, F., . . . Reich, D. (2016). The
608 Simons genome diversity project: 300 genomes from 142 diverse populations. *Nature*,
609 538(7624), 201-206. doi:<https://doi.org/10.1038/nature18964>
- 610 Mathieson, I., Alpaslan-Roodenberg, S., Posth, C., Szecsenyi-Nagy, A., Rohland, N., Mallick, S., . . .
611 Reich, D. (2018). The genomic history of southeastern Europe. *Nature*, 555(7695), 197-203.
612 doi:<https://doi.org/10.1038/nature25778>
- 613 Mathieson, I., Lazaridis, I., Rohland, N., Mallick, S., Patterson, N., Roodenberg, S. A., . . . Reich, D.
614 (2015). Genome-wide patterns of selection in 230 ancient Eurasians. *Nature*, 528(7583), 499-
615 503. doi:<https://doi.org/10.1038/nature16152>
- 616 McColl, H., Racimo, F., Vinner, L., Demeter, F., Gakuhari, T., Moreno-Mayar, J. V., . . . Willerslev, E.
617 (2018). The prehistoric peopling of Southeast Asia. *Science*, 361(6397), 88-92.
618 doi:<https://doi.org/10.1126/science.aat3628>
- 619 McKenna, A., Hanna, M., Banks, E., Sivachenko, A., Cibulskis, K., Kerynsky, A., . . . DePristo, M. A.
620 (2010). The Genome Analysis Toolkit: a MapReduce framework for analyzing next-generation
621 DNA sequencing data. *Genome Research*, 20(9), 1297-1303.
622 doi:<https://doi.org/10.1101/gr.107524.110>
- 623 Moreno-Mayar, J. V., Potter, B. A., Vinner, L., Steinrucken, M., Rasmussen, S., Terhorst, J., . . .
624 Willerslev, E. (2018). Terminal Pleistocene Alaskan genome reveals first founding population
625 of Native Americans. *Nature*, 553(7687), 203-207. doi:<https://doi.org/10.1038/nature25173>
- 626 Narasimhan, V. M., Patterson, N., Moorjani, P., Rohland, N., Bernardos, R., Mallick, S., . . . Reich, D.
627 (2019). The formation of human populations in South and Central Asia. *Science*, 365(6457),
628 eaat7487. doi:<https://doi.org/10.1126/science.aat7487>
- 629 Ning, C., Li, T., Wang, K., Zhang, F., Li, T., Wu, X., . . . Hudson, M. J. J. N. C. (2020). Ancient genomes
630 from northern China suggest links between subsistence changes and human migration. *Nature*
631 *Communications*, 11(1), 1-9. doi:<https://doi.org/10.1038/s41467-020-16557-2>
- 632 Oh, D. S. (2008). Changes in jar coffins of the Honam region. *Journal of The Honam Archaeological*
633 *Society Honam KoKo - Hakbo*, 30(0), 101-138. Korean.
- 634 Park, C.-T. (2010). *On the jar burial of Kyunggi-choongcheong province in 3 ~ 5th Century*. Soongsil
635 University, Seoul, Republic of Korea. (Masters dissertation) Korean.
- 636 Patterson, N., Moorjani, P., Luo, Y., Mallick, S., Rohland, N., Zhan, Y., . . . Reich, D. (2012). Ancient
637 admixture in human history. *Genetics*, 192(3), 1065-1093.
638 doi:<https://doi.org/10.1534/genetics.112.145037>
- 639 Patterson, N., Price, A. L., & Reich, D. (2006). Population structure and eigenanalysis. *PLOS Genetics*,
640 2(12), e190. doi:<https://doi.org/10.1371/journal.pgen.0020190>
- 641 Peltzer, A., Jager, G., Herbig, A., Seitz, A., Kniep, C., Krause, J., & Nieselt, K. (2016). EAGER:
642 efficient ancient genome reconstruction. *Genome Biology*, 17(1), 1-14.
643 doi:<https://doi.org/10.1186/s13059-016-0918-z>
- 644 Poznik, G. D. (2016). Identifying Y-chromosome haplogroups in arbitrarily large samples of sequenced
645 or genotyped men. *bioRxiv*. doi:<https://doi.org/10.1101/088716>
- 646 Raghavan, M., DeGiorgio, M., Albrechtsen, A., Moltke, I., Skoglund, P., Korneliusson, T. S., . . .
647 Willerslev, E. (2014). The genetic prehistory of the New World Arctic. *Science*, 345(6200),
648 1255832. doi:<https://doi.org/10.1126/science.1255832>
- 649 Raghavan, M., Skoglund, P., Graf, K. E., Metspalu, M., Albrechtsen, A., Moltke, I., . . . Willerslev, E.
650 (2014). Upper Palaeolithic Siberian genome reveals dual ancestry of Native Americans. *Nature*,

- 505(7481), 87-91. doi:<https://doi.org/10.1038/nature12736>
- 652 Rasmussen, M., Anzick, S. L., Waters, M. R., Skoglund, P., DeGiorgio, M., Stafford, T. W., Jr., . . .
653 Willerslev, E. (2014). The genome of a Late Pleistocene human from a Clovis burial site in
654 western Montana. *Nature*, 506(7487), 225-229. doi:<https://doi.org/10.1038/nature13025>
- 655 Rasmussen, M., Li, Y., Lindgreen, S., Pedersen, J. S., Albrechtsen, A., Moltke, I., . . . Willerslev, E.
656 (2010). Ancient human genome sequence of an extinct Palaeo-Eskimo. *Nature*, 463(7282), 757-
657 762. doi:<https://doi.org/10.1038/nature08835>
- 658 Rasmussen, M., Sikora, M., Albrechtsen, A., Korneliussen, T. S., Moreno-Mayar, J. V., Poznik, G. D., . . .
659 Willerslev, E. (2015). The ancestry and affiliations of Kennewick Man. *Nature*, 523(7561), 455-
660 458. doi:<https://doi.org/10.1038/nature14625>
- 661 Reich, D., Patterson, N., Campbell, D., Tandon, A., Mazieres, S., Ray, N., . . . Ruiz-Linares, A. (2012).
662 Reconstructing Native American population history. *Nature*, 488(7411), 370-374.
663 doi:<https://doi.org/10.1038/nature11258>
- 664 Renaud, G., Slon, V., Duggan, A. T., & Kelso, J. (2015). Schmutzi: estimation of contamination and
665 endogenous mitochondrial consensus calling for ancient DNA. *Genome Biology*, 16(1), 1-18.
666 doi:<https://doi.org/10.1186/s13059-015-0776-0>
- 667 Ringbauer, H., Novembre, J., & Steinrücken, M. (2020). Human parental relatedness through time-
668 detecting runs of homozygosity in ancient DNA. *bioRxiv*.
669 doi:<https://doi.org/10.1101/2020.05.31.126912>
- 670 Robbeets, M., Bouckaert, R., Conte, M., Savelyev, A., Li, T., An, D. I., . . . Ning, C. (2021).
671 Triangulation supports agricultural spread of the Transeurasian languages. *Nature*, 599(7886),
672 616-621. doi:<https://doi.org/10.1038/s41586-021-04108-8>
- 673 Rohland, N., Harney, E., Mallick, S., Nordenfelt, S., & Reich, D. (2015). Partial uracil-DNA-
674 glycosylase treatment for screening of ancient DNA. *Philosophical Transactions of the Royal
675 Society B: Biological Sciences*, 370(1660), 20130624.
676 doi:<https://doi.org/10.1098/rstb.2013.0624>
- 677 Schubert, M., Lindgreen, S., & Orlando, L. (2016). AdapterRemoval v2: rapid adapter trimming,
678 identification, and read merging. *BMC research notes*, 9(1), 1-7.
679 doi:<https://doi.org/10.1186/s13104-016-1900-2>
- 680 Shewan, L., Armstrong, R., O'Reilly, D., Halcrow, S., Beavan, N., & Sokha, T. (2020). Isotopic insights
681 into the jar-and-coffin mortuary ritual of the Cardamom Mountains, Cambodia. *Antiquity*,
682 94(378), 1575-1591. doi:<https://doi.org/10.15184/aqy.2020.201>
- 683 Sikora, M., Pitulko, V. V., Sousa, V. C., Allentoft, M. E., Vinner, L., Rasmussen, S., . . . Renaud, G.
684 (2019). The population history of northeastern Siberia since the Pleistocene. *Nature*, 570(7760),
685 182-188. doi:<https://doi.org/10.1038/s41586-019-1279-z>
- 686 Sirak, K. A., Fernandes, D. M., Cheronet, O., Novak, M., Gamarra, B., Balassa, T., . . . Pinhasi, R.
687 (2017). A minimally-invasive method for sampling human petrous bones from the cranial base
688 for ancient DNA analysis. *BioTechniques*, 62(6), 283-289.
689 doi:<https://doi.org/10.2144/000114558>
- 690 Ubelaker, D. (1999). *Human skeletal remains: Excavation, analysis, interpretation (Manuals on
691 Archaeology 2)*. Washington: Smithsonian Institution.
- 692 Unterlander, M., Palstra, F., Lazaridis, I., Pilipenko, A., Hofmanova, Z., Gross, M., . . . Burger, J. (2017).
693 Ancestry and demography and descendants of Iron Age nomads of the Eurasian Steppe. *Nature
694 Communications*, 8(1), 1-10. doi:<https://doi.org/10.1038/ncomms14615>
- 695 Wang, C.-C., Yeh, H.-Y., Popov, A. N., Zhang, H.-Q., Matsumura, H., Sirak, K., . . . Kim, A. M. (2020).
696 The genomic formation of human populations in East Asia. *bioRxiv*.
697 doi:<https://doi.org/10.1101/2020.03.25.004606>
- 698 Wang, T., Wang, W., Xie, G., Li, Z., Fan, X., Yang, Q., . . . Yang, R. (2021). Human population history
699 at the crossroads of East and Southeast Asia since 11,000 years ago. *Cell*, 184(14), 3829-3841.
700 doi:<https://doi.org/10.1016/j.cell.2021.05.018>
- 701 Weissensteiner, H., Pacher, D., Kloss-Brandstatter, A., Forer, L., Specht, G., Bandelt, H. J., . . .
702 Schonherr, S. (2016). HaploGrep 2: mitochondrial haplogroup classification in the era of high-
703 throughput sequencing. *Nucleic Acids Research*, 44(W1), W58-63.
704 doi:<https://doi.org/10.1093/nar/gkw233>
- 705 White, T. D., & Folkens, P. A. (2005). *The human bone manual*. Amsterdam: Academic Press.

- 706 White, T. E. (1953). A method of calculating the dietary percentage of various food animals utilized by
707 aboriginal peoples. *American Antiquity*, 18(4), 396-398. doi:<https://doi.org/10.2307/277116>
- 708 Yang, M. A., Fan, X., Sun, B., Chen, C., Lang, J., Ko, Y. C., . . . Fu, Q. (2020). Ancient DNA indicates
709 human population shifts and admixture in northern and southern China. *Science*, 369(6501),
710 282-288. doi:<https://doi.org/10.1126/science.aba0909>
- 711 Yang, M. A., Gao, X., Theunert, C., Tong, H., Aximu-Petri, A., Nickel, B., . . . Kelso, J. (2017). 40,000-
712 year-old individual from Asia provides insight into early population structure in Eurasia.
713 *Current Biology*, 27(20), 3202-3208. doi:<https://doi.org/10.1016/j.cub.2017.09.030>
- 714 Yu, H., Spyrou, M. A., Karapetian, M., Shnaider, S., Radzeviciute, R., Nagele, K., . . . Krause, J. (2020).
715 Paleolithic to Bronze Age Siberians reveal connections with first Americans and across Eurasia.
716 *Cell*, 181(6), 1232-1245. doi:<https://doi.org/10.1016/j.cell.2020.04.037>
- 717
718
719